

Bistatic system and baseline calibration in TanDEM-X to ensure the global digital elevation model quality

Jaime Hueso González*, John Mohan Walter Antony, Markus Bachmann, Gerhard Krieger, Manfred Zink, Dirk Schrank, Marco Schwerdt

German Aerospace Center (DLR), Microwaves and Radar Institute (HR), 82234 Wessling, Germany

ARTICLE INFO

Article history:

Available online 18 June 2012

Keywords:

Accuracy
Calibration
Digital
Interferometer
SAR
Satellite
Space

ABSTRACT

TanDEM-X is an operational satellite mission with the goal of generating a high quality global digital elevation model (DEM) based on synthetic aperture radar (SAR) interferometry in X-band. In order to ensure the quality of the DEM, the differential range measurements and knowledge of the interferometric baseline have to be extremely accurate. In this paper, the bistatic system calibration strategy implemented in TanDEM-X to achieve the desired DEM quality will be described, focusing on the baseline calibration procedure. The results of the tests, which were performed in parallel to the operational DEM acquisition, verify the suitability of this approach.

© 2012 International Society for Photogrammetry and Remote Sensing, Inc. (ISPRS) Published by Elsevier B.V. All rights reserved.

1. Introduction

The currently operational TanDEM-X mission (Krieger et al., 2007) consists of two twin satellites provided with X-band SAR instruments, TerraSAR-X (TSX) and TanDEM-X (TDX), flying in a controlled helix formation, with typical baseline lengths of 250–1000 m. This configuration enables the systematic acquisition of single-pass cross-track interferograms of the Earth, in the pursuit of generating a high quality global DEM. This mission is implemented in the framework of a public–private partnership between the German Aerospace Center (DLR) and Astrium GmbH. TDX was launched into orbit in June 2010, joining TSX, already operational since 2007. During the summer of 2010, the first part of the commissioning phase took place, in which both satellites were arranged in a safe 20-km distance pursuit monostatic formation, in order to calibrate TDX for the monostatic operation. In October 2010, the mean along-track distance was eliminated and both satellites started to orbit in a close helix formation. This was also the beginning of the so-called bistatic commissioning phase, where different bistatic issues were tested (Hueso González et al., 2010c). 2 months later, in mid December, the nominal DEM data acquisition started in order to fulfill the mission schedule. However, some calibration activities continued in parallel to monitor this complex system, and to store vital information for the health of the mission, like the aspects related to DEM calibration. In order

to ensure the quality of the DEM, the differential range measurements have to be precise enough to avoid missing the right interferometric ambiguity interval. The accuracy in the knowledge of the baseline between the two satellites is critical, as well, since it has a direct impact on the final DEM quality.

This paper is structured as follows. After this introduction, Section 2 describes the driving requirements related to the DEM accuracy, and the flow of the DEM calibration processing chain. These requirements motivate the development of the calibration procedures also mentioned here. Section 3 focuses on the baseline problematic and describes the impact of this potential error on the resulting DEM. In Section 4, the algorithm to compensate the baseline errors is described in detail. The measurements of the operational mission will be shown in Section 5, which verify the suitability of this approach. Finally, Section 6 summarizes all the corrections applied to the system and evaluates the fulfillment of the requirements of this highly complex radar imaging mission, prior to the final DEM calibration and mosaicking process (Hueso González et al., 2010a).

2. TanDEM-X driving requirements

2.1. DEM calibration flow

In early mission design stages, it was assumed that the knowledge of the baseline vector between TSX and TDX, as provided by differential GPS measurements, was accurate enough to result in moderate systematic height errors that could be cancelled by

* Corresponding author.

E-mail address: desperta@yahoo.com (J. Hueso González).

applying the foreseen mosaicking algorithms (Hueso González et al., 2010a). However, dedicated studies on this issue have shown that a baseline bias in the order of 1–10 mm cannot be excluded, as it will be explained in Section 3. Therefore, the existing processing and calibration concept had to be extended to take into account a more realistic scenario, as shown in Table 1.

The final objective is to have a global DEM with a relative height accuracy of 2 m (and 10 m absolute), which is achieved in the DEM mosaicking and calibration processor. This is only possible if a series of pre-requisites or pre-requirements are fulfilled, as represented in the row “Driving accuracy goal” of Table 1.

First, a baseline product based on GPS navigation data is needed to process the TanDEM-X raw DEMs (“raw” means before baseline and DEM calibration). The maximum acceptable error of this baseline is a bias of up to 10 mm, with little variation over time. Since there are different algorithms to obtain the baseline (see Section 2.2), several of them have been tested for identifying the best performance for TanDEM-X. Once an accurate baseline is available, the raw DEMs are processed. For this, one should be aware that TanDEM-X employs a dedicated bi-directional synchronization link between the two SAR instruments. This enables, in contrast to conventional repeat-pass interferometry, the accurate determination of the interferometric phase, up to an ambiguity of 2π (or 1π , cf. Section 5.3). In order to resolve this residual ambiguity without reference to an external DEM, a second TanDEM-X DEM is generated by radargrammetry, which evaluates the range difference between the co-registered mono- and bistatic SAR images. The radargrammetric DEM is unambiguous, but its accuracy is strongly limited by the range bandwidth, leading to a height accuracy that is typically two to three orders of magnitude worse than its interferometric counterpart (Bamler and Eineder, 2005). By evaluating large areas, the height accuracy of the radargrammetric DEM is nevertheless sufficient to resolve the unknown ambiguity interval in the interferometric DEM, and such a strategy has been implemented in the operational TanDEM-X DEM processor. From this, the new requirement arises that the radargrammetric range shift measurements have to be accurate within ± 7.5 mm. This demanding requirement imposes in turn a set of additional requirements on the knowledge of the differential delays in both the radar signal and the bidirectional synchronization path. Section 2.2 will deal with the measurement and compensation of these delays.

After correcting the additional delays, the baseline bias can be monitored and characterized by means of a comparison of a representative set of selected raw DEMs with external references. Finally, the calibrated baseline is generated and used for operational DEM generation. The calibrated baseline will only have a residual random error, and is supposed to have an accuracy of 1–2 mm. In Fig. 1, an example of the height error histograms of the DEMs in the different calibration stages is shown. The red curve represents the errors in the raw DEM before baseline calibration, and the green curve is the same DEM re-processed with the calibrated baseline. The elimination of the height error offset can be clearly seen (simultaneously, a ground range displacement not depicted in this graphic has also been cancelled).

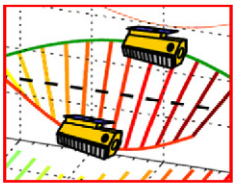
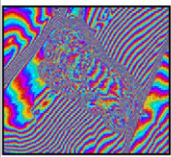
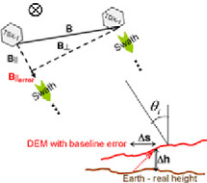
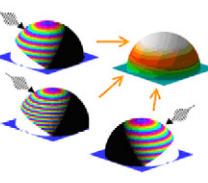

Since we are not dealing with individual DEMs, but with multiple adjacent and crossing long DEM stripes, the last two calibration methods depicted in Table 1 exploit the additional information provided by the overlapping or connected DEMs. A special acquisition plan over three years has been established to provide multiple acquisitions over the whole Earth surface (Krieger et al., 2007). The different acquisitions, depending on the Earth region, have different height of ambiguities or acquisition geometries, which allows the implementation of a dual- or multi-baseline phase unwrapping algorithm (Lachaise et al., 2008) to minimize phase unwrapping errors, layover and shadowing effects.

After all these steps, these are the DEM products that enter the final DEM calibration and mosaicking process. Here, ICESat points are used as height references (Abshire et al., 2005; Hueso González et al., 2010b), with an absolute accuracy better than 0.5 m. The result is exemplarily shown in the yellow histogram of Fig. 1, which fulfills the challenging TanDEM-X global DEM accuracy expectations. Note that we expect from the full calibration workflow an absolute DEM height accuracy much better than the 10 m specification.

2.2. Methods to achieve the requirements

The calibration steps described in Section 2.1 are executed by means of different methods and algorithms. Some of them have already been documented in the literature, thus we will only mention the existing references in these cases, while focusing on the rest of them.

Table 1
DEM calibration workflow of the TanDEM-X mission. Columns represent the different steps in the processing chain, and the arrows indicate the logical order in the chain. “DT” stands for data take (column “Precise Baseline”).

Products	Precise Baseline	Raw DEM	Calibrated Baseline	Multiple Acquisitions	Final DEM
Driving accuracy goal	Baseline error <10 mm (bias) 3 helix coordinate components error – constant over typical DT	Absolute phase determination ± 7.5 mm radargram. accuracy	Baseline error 1–2 mm (1σ)	Minimize phase unwrapping, shadowing and layover	Relative height accuracy 2 m (90%)
Method to achieve it	Baseline determination GFZ: EPOS, BERNESE DLR: FRNS	Radargrammetric delay compensation bistatic processing	Baseline Calibration weightings, height error determination, maneuvers	Multi-baseline phase unwrapping 3-years acquisition plan	DEM mosaicking and calibration
					

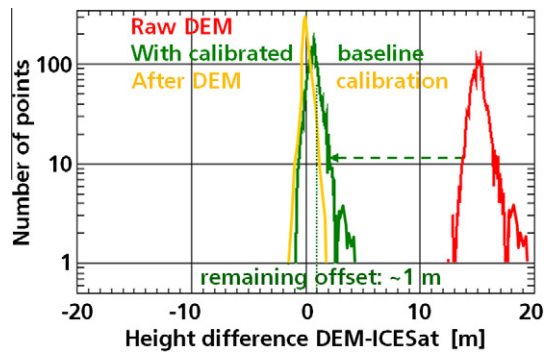


Fig. 1. Histograms corresponding to the height errors of the different intermediate DEM products after each calibration step.

The TanDEM-X orbit product is based on information provided by the on-board GPS receivers, called TOR/IGOR System (Tracking, Occultation and Ranging/Integrated GPS Occultation Receiver) (Montenbruck et al., 2011). The precise baseline is derived from double differential GPS (DDGPS) carrier phase measurements between both satellites and applying a Kalman filter method to the data. The use of the differential information even eliminates ionospheric errors and other characteristic GPS perturbations. Several algorithms exist for calculating the baseline from these data:

- Earth Parameter and Orbit determination System (EPOS-OC) (Zhu et al., 2004).
- Bernese (Beutler et al., 2007).
- Filter for Relative Navigation of Spacecraft (FRNS) (Kroes, 2006; Montenbruck et al., 2011).

Two baseline products are generated with the first two methods by the GeoForschungsZentrum Potsdam (GFZ), and a third one with FRNS by the German Space Operations Center (GSOC) at DLR. Verification results in a selected set of test sites prove that the three products fulfill the requirement of 10 mm accuracy, with the exception of some outliers, usually originated close to (within 30 min around) satellite maneuvers, which take place generally once a day. The outliers do not usually occur simultaneously on all products. Therefore, a suitable combination of the different products is applied to temporarily mask the inaccurate baseline values.

Once the precise baseline accuracy is ensured, the DEMs have to be processed in a special way, so that the absolute phase can be determined without the aid of external height references (Bamler and Eineder, 2005). This algorithm is very sensitive to delays in the radar signal, hence requiring a radargrammetric accuracy of

± 7.5 mm. Fig. 2 is a plot of the differential radargrammetric shifts that have been obtained by comparing TanDEM-X radargrammetric DEMs with those of the SRTM mission. It shows the necessity of applying delay corrections on the data before continuing with the DEM calibration process, since more than half of the measurements fall out of the target interval. The dependence on the argument of latitude and on the satellite that acts as “master” in the DEM acquisition indicates that these delays are probably related to instrument effects and processing aspects affected by the orbit position of the satellites. Note that “argument of latitude” is an angular parameter equal to the true anomaly plus the argument of periapsis: values of 0° and 180° correspond to equator crossings of the satellite ground track, whereas 90° and 270° are near the North and South Poles, respectively.

After thorough analysis, the following sources of uncompensated differential range shifts were identified:

- Unbalanced global internal delays of both satellites.
- Internal delays dependent on the chirp bandwidth.
- Internal delays dependent on the synchronization horn configuration.
- Different internal delays of the instrument depending on the configuration of the attenuator elements (RxGain).
- Relativistic effects on the time references of both satellites, dependent on the relative position (with a periodicity of one orbit), and affecting among other aspects the processing of the pulses in the synchronization signal exchange between TSX and TDX (Krieger et al., 2007).

In the frame of geometric calibration acquisitions over corner reflectors during the TDX monostatic commissioning phase (Schwerdt et al., 2011), a precise internal delay (mean residual range error) could be measured: 212.1998 ns for TDX, and 212.1199 ns for TSX. The standard deviation of the measurements is 0.72 ns, which corresponds to a geometric standard deviation of around 10 cm. The application of these values in the processing improved the first approximation, which assumed that the delay of TDX was the same as the one of TSX. However, the performed corner measurements estimate the monostatic instrument delays. Since no measurements of the bistatic instrument delay were available, it was decided to use the monostatic delay of the passive satellite instead. Two additional delay correction values were derived empirically to compensate the error of this approximation. Thus, the differential delay is eliminated in the radargrammetric shift plot (see Fig. 3).

Another experiment was performed in which several consecutive acquisitions (or DTs) with equal commanding parameters were performed, just by changing the chirp bandwidth. The results show a relatively stable shift between the 100 MHz and the 150 MHz configuration (Fig. 4).

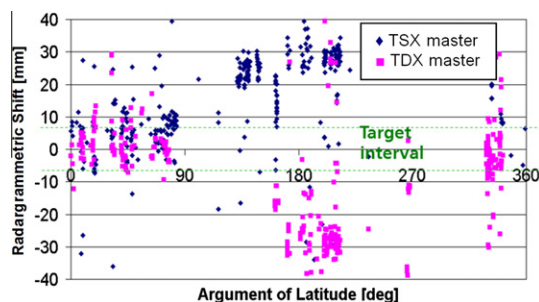


Fig. 2. Estimated radargrammetric shifts of the TanDEM-X DEMs with respect to the ones derived with the help of SRTM, before applying correction parameters, in terms of the argument of latitude. Points outside the target interval indicate interferograms with ambiguous phase.

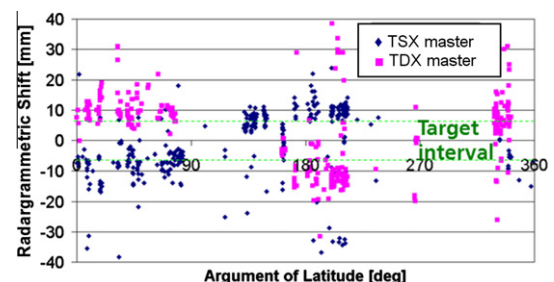


Fig. 3. Estimated radargrammetric shifts after correction of the differential instrument delays.

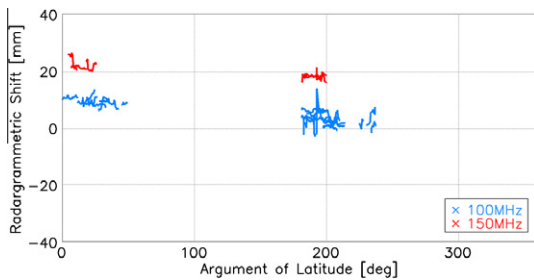


Fig. 4. Test to identify the impact of the chirp bandwidth on the radargrammetric shifts.

An analog test dealt with the choice of the active synchronization horn combination (Krieger et al., 2007). Offsets in the shifts could be directly detected between the different possible horn pairs (see Fig. 5).

A further experiment consisted of a calibration data take with a sweep of the attenuator configurations (from 0 to 30 dB). The differential delay of the internal electronics was calculated by compressing the calibration pulses and estimating the instant of arrival of the pulse peak. Fig. 6 (right) summarizes the results of these measurements for TSX. The highest jump in the delay happens between the 14 dB and the 16 dB configuration, due to the internal construction of the attenuator device (left-hand side of Fig. 6). In that particular transition, all the switches change their state. Since these delays are different for TDX, the change of the RxGain configuration between TanDEM-X acquisitions caused differential delay changes.

The effects described here (Figs. 4–6) are compensated before the raw DEM generation by means of ground segment correction tables.

Another interesting contribution to the delay was identified during the TanDEM-X commissioning phase. It is a relativistic effect (first time empirically measured in a real satellite constellation) due to the use of different reference frames: one for radar synchronization, which is performed in a satellite reference system, and the other for bistatic SAR processing, which is performed in an Earth Centered Earth Fixed reference frame. The practical impact on the radargrammetric shifts is an orbit-dependent sinusoidal displacement of the measurements (see Fig. 7), with opposite

sign dependent on which satellite is acting as “master”. A detailed description of the mathematics of these relativistic corrections, implemented now in the TanDEM-X processor, is out of the scope of this article, but will be the subject of future publications.

Finally, Fig. 8 shows the estimated the radargrammetric shifts for a subset of the data after all the identified corrections have been applied. Since almost all shifts fall within the target interval, this proves the validity of the adopted approach for the achievement of the raw DEM accuracy objectives.

Section 4 will focus on the algorithms for the baseline calibration. The implementations of the multi-baseline phase unwrapping approach and of the DEM calibration are broadly described in (Lachaise et al., 2008) and (Hueso González et al., 2010a), respectively.

3. Baseline problematic

The initial baseline determination accuracy expectations (1 mm accuracy) were based on the performance of the DDGPS method in similar missions like GRACE (Kroes et al., 2005). The comparison is possible since GRACE is also a two satellite formation with similar orbit period, GPS receivers and baseline determination methods (DDGPS relative navigation) as the TanDEM-X formation. The baseline error in the GRACE formation was estimated by comparing the GPS-processed data with the highly accurate measurements from a dedicated on-board Ka-band link (see Fig. 9).

The results in TanDEM-X should be better than in GRACE as the baseline length is much shorter and the GPS receivers have a slightly better performance. However, GRACE results do not prove that the 1 mm baseline accuracy is reached in absolute terms, i.e., it may be subject to a constant bias of several mm (see sketch of such a bias in Fig. 10), since the Ka-band measurement system might have phase ambiguities. For this, the TanDEM-X DEM calibration has a cautious approach and considers the possibility of having a small offset or “bias” in the baseline product in the order of 2–10 mm. Such an offset could be due to small measurement errors in the location of the baseline reference points in the satellite payload, or small systematic errors of the DDGPS measurements, or other unknown reasons (in the case of GRACE, hidden by a constant number of phase ambiguities). Although, the experience in GRACE suggests that it should be almost constant over time, since the measurements shown in Fig. 9 do not experiment jumps that could

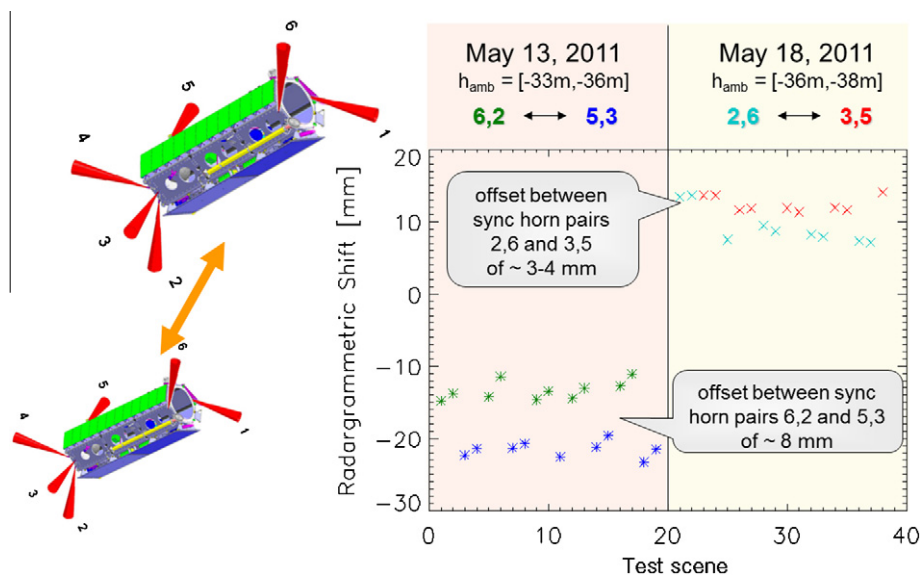


Fig. 5. Test to identify the impact of the synchronization horn combination on the radargrammetric shifts.

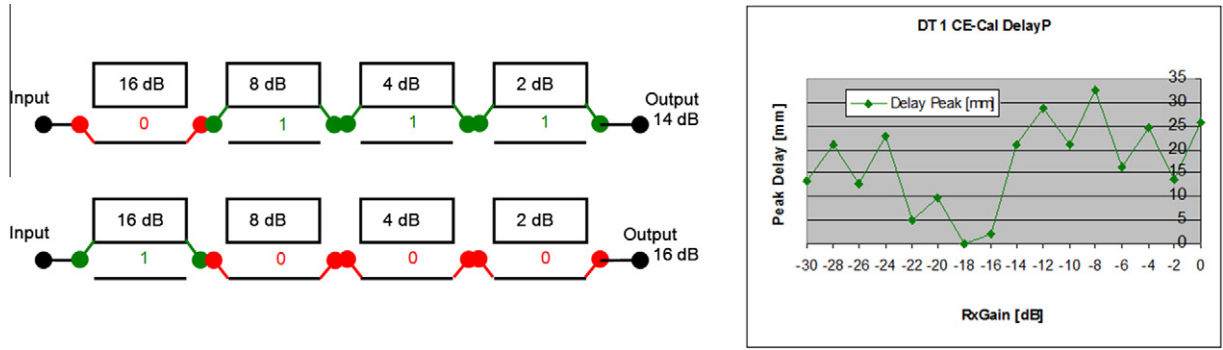


Fig. 6. Left: Scheme of the RxGain attenuator. The switches are set for 14 dB (upper) and 16 dB (lower) attenuation. Right: Measured delays from an internal test to identify the impact of the attenuator (RxGain) configuration on the signal delay in the instrument electronics.

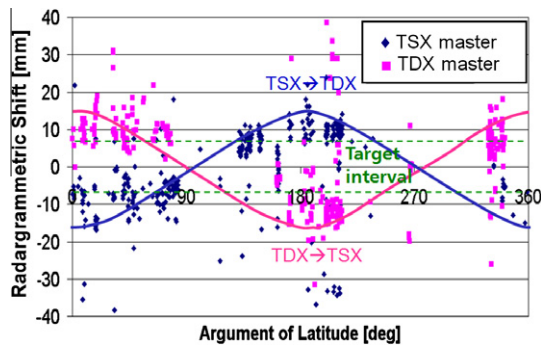


Fig. 7. Impact of the relativistic effect on the radargrammetric shifts.

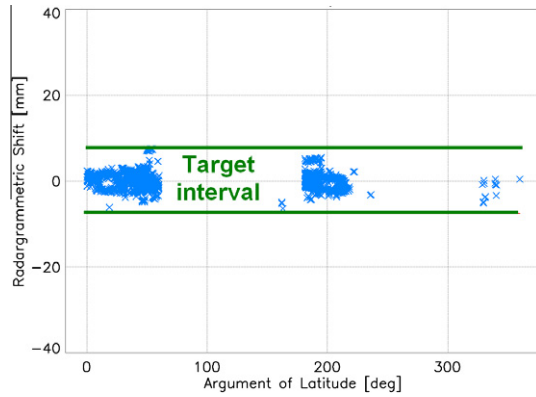


Fig. 8. Estimated radargrammetric shifts after correction of all identified contributions for a subset of TanDEM-X acquisitions.

be associated with phase-wrapping effects over the whole time period (around one day).

Considering a 3D baseline error vector, the strongest effect in the DEM height is caused by the component parallel to the line-of-sight (LOS) $B_{||err}$ (bistatic operation):

$$h_{err} = \frac{r \sin(\theta_i)}{B_{\perp}} \cdot B_{||err} \quad (1)$$

where r is the slant range distance to the target, θ_i the incidence angle with respect to the nadir vector at target position and B_{\perp} the component of the baseline vector perpendicular to the LOS, as shown in Fig. 11.

In fact, a $B_{||err}$ causes a rotation of the DEM around the flight trajectory, so the height error is always linked to a ground range displacement gr_{err} :

$$gr_{err} = \frac{r \cos(\theta_i)}{B_{\perp}} \cdot B_{||err} \quad (2)$$

The presence of a relatively high bias in the baseline knowledge (compared with the 1 mm relative baseline accuracy) is therefore reflected in a considerable height and ground range displacement error in the raw DEMs. Simple height offsets could be corrected by the vertical corrections in the DEM calibration process, but this would not solve the ground range shifts of the DEMs. This could mean that, when applying height references to calibrate the DEM, they would be placed in locations shifted in ground range direction, introducing additional height errors that could endanger the global DEM height quality. Therefore, a solution is searched to minimize potential baseline offsets and eliminate this problematic before starting the DEM calibration process.

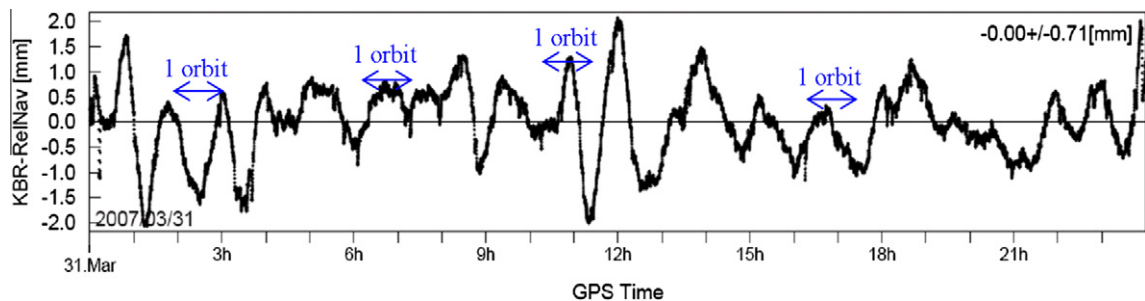


Fig. 9. One day comparison between Ka-band and DDGPS baselines by GRACE. Orbit period ~ 90 min. Standard deviation of the error is $0.71 \text{ mm} < 1 \text{ mm}$. Source: Wermuth/Montenbruck (GSOC-DLR).

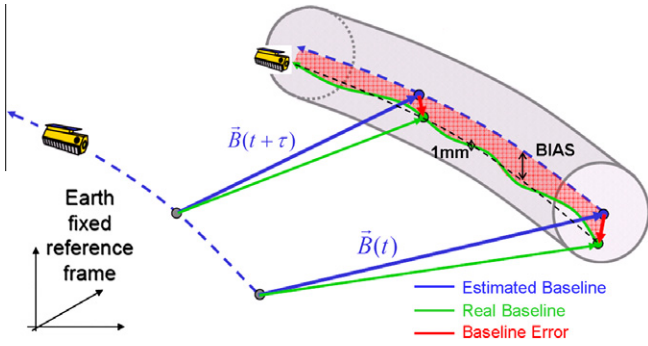


Fig. 10. TanDEM-X mission baseline error evolution over time.

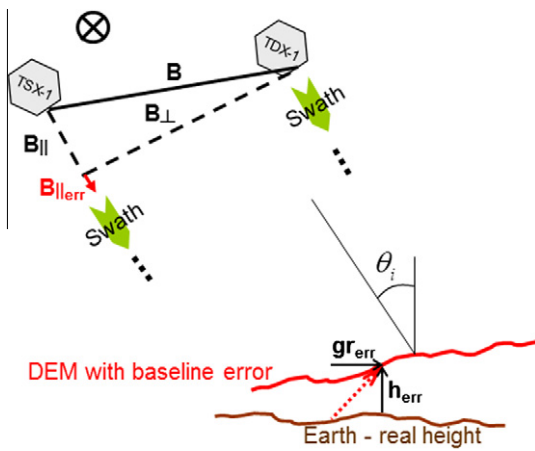


Fig. 11. Effects of a baseline LOS error on the DEM. Circle with a cross indicates flight direction into the image.

4. Baseline calibration algorithm

4.1. Height error determination

The main contribution to the height error is caused by the baseline error in LOS. In the presence of a baseline bias in LOS larger than 2 mm, it is justified to assume that this is the only significant source of the systematic height error in a raw DEM (Hueso González et al. 2010a). As explained in previous sections, this approach assumes that the raw DEM was generated by applying absolute phase techniques. Following this philosophy, a simple characterization strategy for the baseline bias has been proposed. For a given raw DEM over a region with accurate height references, the baseline offset in LOS at the time of the acquisition can be estimated through interferometry. The height difference observed is introduced in (1) and the unknown $B_{\parallel \text{err}}$ calculated. As the baseline bias is expected to be relatively constant, an average height error value should be sufficient to derive the $B_{\parallel \text{err}}$ estimate. Fig. 12 illustrates such an average height determination. Over a certain DEM, the high quality ICESat points – or SRTM (Carabajal and Harding, 2006) combined with ICESat – are selected as described in (Hueso González et al., 2010b). The average height error is directly obtained.

4.2. 2D helix relative baseline offset compensation

A proper distribution of test sites over the world is necessary to characterize the baseline bias vector. Test regions have been identified over the whole world to allow constant monitoring and characterization of the baseline during the commissioning phase and further on in the operational mission, with around 2–6 acquisitions per day. The test sites correspond to extremely flat regions, to avoid the coupling of ground range displacement with height errors, and with little vegetation, where the height references are most reliable (see an example on the left-hand side of Fig. 13). They are large enough to contain consecutive acquisitions of two or three short DTs in the same overflight (see right-hand side of Fig. 13). Each of these DTs provides a height difference that can be converted in a one-dimensional baseline LOS error. But we need

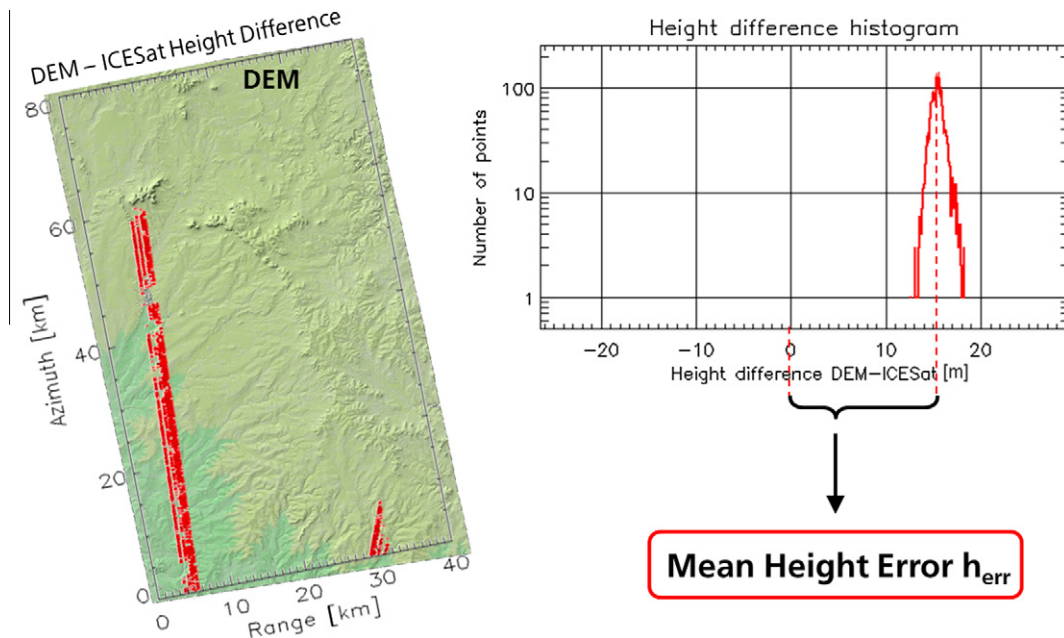


Fig. 12. Illustration of the mean height error estimation method with the help of ICESat height references.

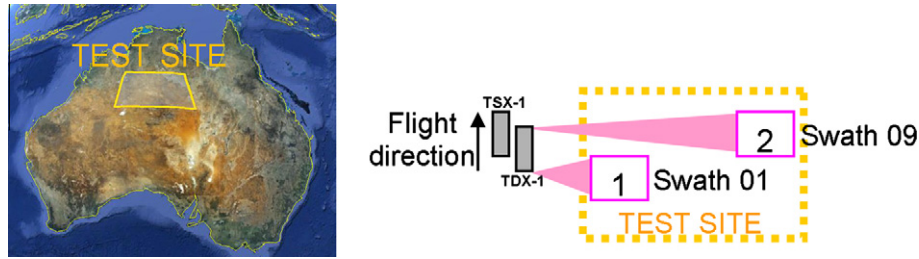


Fig. 13. Acquisition of consecutive swaths with maximal and minimal incidence angle swaths for obtaining the 2D baseline error vector.

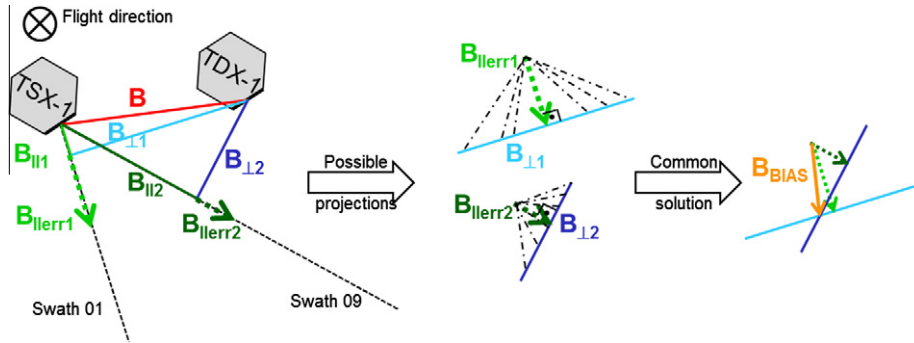


Fig. 14. Derivation of the 2D baseline bias error vector from two one-dimensional error estimations.

Table 2

Summary of the correction parameters applied to improve the radargrammetric shifts of the TanDEM-X data. Exact values depend on the particular instrument configuration. “Y(es)” and “N(o)” indicate whether the contribution has an impact or not on the radargrammetric shift or the interferometric phase.

Contribution/dependency	Applied correction	Radargr. shift	Phase
Bistatic internal delay imbalance	TSX: 2mmTDX: -7 mm	Y	N
Relativistic effects	Along-track dependent	Y	Y
Sync horn pair	0 to ± 13 mm	Y	N
Bandwidth 100 ⇔ 150 MHz	±12 mm	Y	N
Rx gain	0 to ± 13 mm	Y	N

interferometric images different incidence angles. The incidence angles should be as different as possible within the full performance range of the SAR antenna, e.g. near range (swath 01, with an incidence angle 31°) and far range (swath 09, with an incidence angle of 48°). Based on Section 3, we reasonably assume that the eventual baseline error remains constant over the 30 s that the operation of acquiring these two consecutive DTs over the same test site approximately lasts. By a simple geometrical calculation, illustrated in Fig. 14, the baseline bias vector in the plane perpendicular to the flight direction is derived from this pair (or trio) of DEM acquisitions with different swaths.

The operation of Fig. 14 can also be expressed mathematically as follows:

$$\vec{B}_{BIAS} = \vec{B}_{err||1} + k_1 \cdot \hat{B}_{\perp 1} = \vec{B}_{err||2} + k_2 \cdot \hat{B}_{\perp 2} \quad (3)$$

a two-dimensional projection of the true baseline error vector in the plane perpendicular to the flight direction (B_{BIAS}), which are the components that affect the height accuracy of the DEM. The way to achieve this is by selecting for each of the two consecutive

where \hat{B}_{\perp} is a unitary vector perpendicular to the line-of-sight (=perpendicular baseline unitary vector), and k_1, k_2 are real variables that can be obtained by solving this linear system.

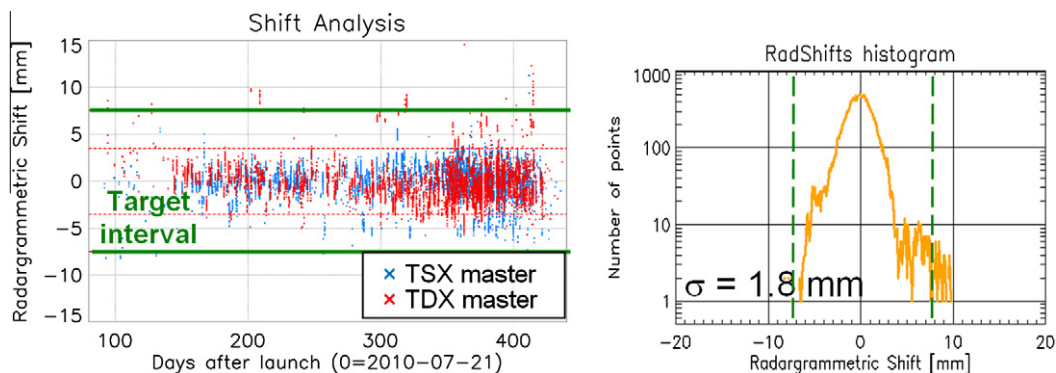


Fig. 15. Estimated radargrammetric shifts of the TanDEM-X DEMs with respect to the ones derived with the help of SRTM, after applying the correction parameters derived in this paper. Left: Plot over time. Right: Histogram and standard deviation.

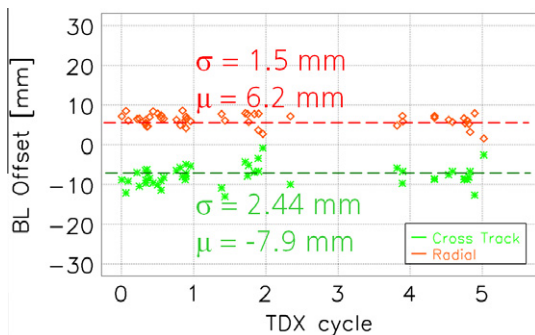


Fig. 16. 2D helix relative baseline error components of the TanDEM-X DEMs in the pursuit monostatic commissioning phase before baseline calibration. The offset can be clearly detected. No systematic was found over the orbit or over the argument of latitude.

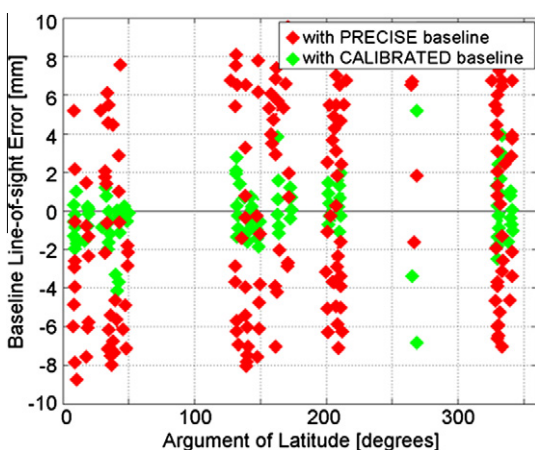


Fig. 17. Line-of-sight baseline error of the TanDEM-X DEMs in the pursuit monostatic commissioning phase over argument of latitude before and after baseline calibration.

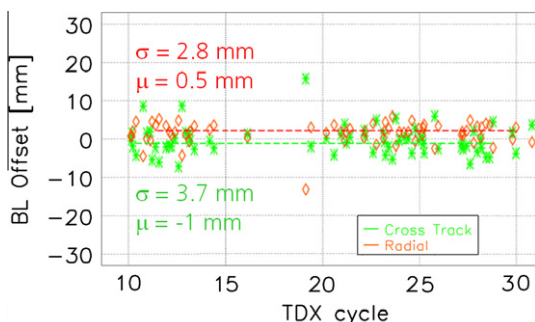


Fig. 18. 2D helix relative baseline error components of the TanDEM-X DEMs in the bistatic commissioning phase and the operational mission before baseline calibration.

5. Experimental results and current mission status

5.1. Radargrammetric shift

During both the commissioning phase and the operational DEM acquisition of TanDEM-X, the radargrammetric shifts of all acquisitions are monitored. After applying all the corrections summarized in Table 2, the results from 17,000 DEMs are plotted in Fig. 15, which demonstrates that the requirements (target interval) defined in Section 2 are fulfilled (compare with Figs. 2 and 8) in

Table 3

Statistics of the radargrammetric and height difference with SRTM (and other references) of the operationally processed TanDEM-X DEMs until October 2011. “Active” defines which of the satellites acts as master in the bistatic SAR acquisition.

	Number of processed scenes	Shifts < 7.50 mm (%)	Shifts < 3.50 mm (%)	DEM-SRTM < 10 m (%)
TSX active	9000	99.8	95.1	89.6
TDX active	9000	99.4	94.9	88.4
Total	18,000	99.6	95	89

almost all cases and the standard deviation is 1.8 mm. Table 2 also indicates that all contributions have an impact on the radargrammetric shift, but only the relativistic effect has a noticeable influence on the interferometric phase.

5.2. Baseline calibration in the pursuit monostatic phase

During the monostatic commissioning phase, TSX and TDX were flying at an approximate along-track distance of 20 km and operated in pursuit monostatic mode. Around three characterisations, each of them consisting of two or three acquisitions with minimum, intermediate and maximum incidence angle swaths (cf. Fig. 13), were performed every day. The test sites were well distributed over the world, hence allowing the identification of a potential systematic of the error over the argument of latitude. However, the detected offset (μ in Fig. 16) was very constant over time and argument of latitude, with a value of -7.9 mm in cross-track and 6.2 mm in radial direction for the DLR FRNS product. The σ or standard deviation values give an order of magnitude of the precision achievable with this characterization method.

Once this offset was applied to the data, the LOS errors detected in the test sites were considerably reduced (see Fig. 17), reaching the accuracy required by the mission of around 1 mm (1σ). Taking into account that this standard deviation includes also residual errors from the reference DEMs, these results were considered as very promising.

5.3. Baseline calibration in the bistatic operation

Approximately 90 days after the TDX launch, the satellites were set in a close bistatic formation. The baseline calibration activities continued, and new correction values were identified (see Fig. 18), e.g. for the DLR FRNS baseline, which are different from the ones in the pursuit monostatic phase (cf. Fig. 16).

The exact reason for this discrepancy is still under investigation. One possible explanation is that there are still some phase contributions of the synchronization link processing chain that introduce an offset in the interferograms, and this one is detected by the TanDEM-X calibration approach as a pure baseline offset, thus interfering with the real one. On the other hand, there is a π -ambiguity in the interferogram phases, which is resolved by means of a correction table in the processing stage (in Fig. 18, the phase bands with a π -ambiguity have already been merged). The cause of this error is in the synchronization link processing, which combines the sum of two synchronization phases, one from each satellite, in a common average. Several proposals to eliminate this ambiguity are currently under study.

However, what is more important for the mission is that the baseline offset is very constant over time, hence it can be calibrated out. The statistics of the TanDEM-X mission acquisitions give excellent results in terms of the height comparisons between the DEMs after baseline calibration and SRTM (adjusted with ICESat and complemented by other height databases to fill gaps in high latitudes), as can be seen in Table 3.

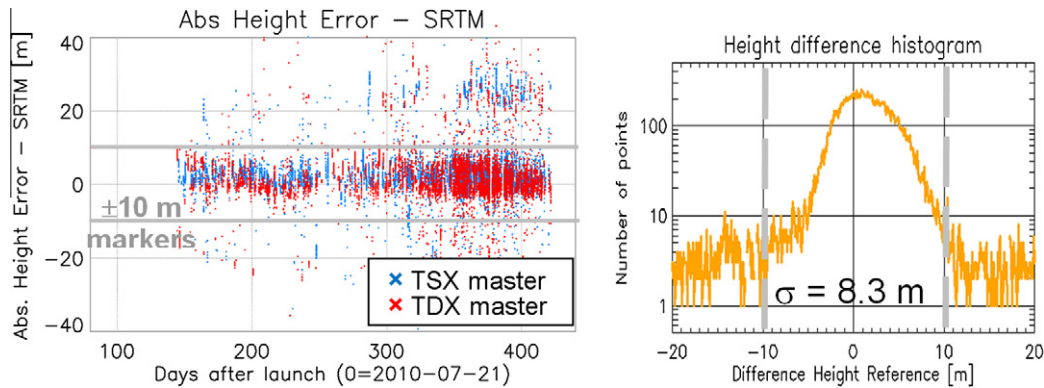


Fig. 19. Absolute height difference between the TanDEM-X DEMs and SRTM (and other references) after correction of the radargrammetric shifts and the calibration of the baseline in bistatic operation. Left: Plot over time. Right: Histogram and standard deviation.

99.6% of the data takes fulfill the radargrammetric shift requirement, whereas around 89% of the DEMs after baseline calibration have an average difference with SRTM of less than 10 m, and with a standard deviation of 8.3 m (cf. also Fig. 19). It has to be noted that the height errors of SRTM and of the complementary databases have also a certain influence on this statistic, and it is expected that the real TanDEM-X errors are even lower, even before the DEM calibration stage, hence keeping the ground range displacements under control. The outliers are automatically detected by comparing adjacent data takes and re-processed. This is an excellent perspective for the next steps towards the TanDEM-X final DEM product.

6. Conclusion

The whole DEM calibration flow in the TanDEM-X mission has been presented in this paper, including the logical steps, requirements and methods needed to achieve the global DEM accuracy objectives. In some cases, the preliminary design had to be extended to cope with the practical complexities of real data processing, and the corresponding test campaigns were organized and successfully executed.

The three available baseline product types have been presented, as well as the strategy to combine them to solve inaccuracies close to manoeuvres. Several delay correction tables have been created to compensate for instrument delays dependent on the satellite commanding and instrument configuration. Furthermore, several updates were undertaken in the processor to consider orbit-dependent relativistic effects and several refinements in the synchronization link. Special emphasis has been put on the baseline calibration procedure, which has a considerable impact on the DEM processing chain and involves almost the whole ground segment.

The characterization measurements over globally distributed test sites have been presented, and the results show a good agreement with the requirements in all processing stages. Some work has still to be done to investigate the source of the inaccuracies in the processing of the synchronization pulses (e.g. the π -ambiguity of the synchronization link phase), which however do not seriously affect the final accuracy of the characterization. This enabled the recent kick-off of the operational DEM production. As a summary, the current status gives very promising perspectives for the TanDEM-X mission, which is entering with full confidence the also challenging multi-baseline processing and DEM mosaicking stages.

Acknowledgements

The authors would like to thank the whole TanDEM-X Ground Segment team at DLR (acquisition planning, commanding, flight operations, baseline generation, processing, calibration, mosaicking) for their cooperation during these months in the different working groups and their extraordinary efforts for bringing forward this challenging mission. The TanDEM-X project is partly funded by the German Federal Ministry for Economics and Technology (Förderkennzeichen 50 EE 1035).

References

- Abshire, J.B., Sun, X., Riris, H., Sirota, J.M., McGarry, J.F., Palm, S., Yi, D., Liiva, P., 2005. Geoscience laser altimeter system (GLAS) on the ICESat mission: on-orbit measurement performance. *Geophysical Research Letters* 32 (L21S02).
- Bamler, R., Eineder, M., 2005. Accuracy of differential shift estimation by correlation and split-bandwidth interferometry for wideband and delta-k SAR systems. *IEEE Geoscience and Remote Sensing Letters* 2 (2), 152–155.
- Beutler, G., Bock, H., Dach, R., Fridez, P., Gaede, A., Hugentobler, U., Jaeggi, A., Meindl, M., Mervart, L., Prange, L., Schaer, S., Springer, T., Urschl, C., Walser, P., 2007. Bernese GPS Software, Version 5.0. Astronomical Institute, University of Bern.
- Carabajal, C., Harding, D., 2006. SRTM C-band and ICESat laser altimetry elevation comparisons as a function of tree cover and relief. *Photogrammetric Engineering & Remote Sensing* 72 (3), 287–298.
- Hueso González, J., Bachmann, M., Krieger, G., Fiedler, H., 2010a. Development of the TanDEM-X calibration concept: analysis of systematic errors. *IEEE Transactions on Geoscience and Remote Sensing* 48 (2), 716–726.
- Hueso González, J., Bachmann, M., Scheiber, R., Krieger, G., 2010b. Definition of ICESat selection criteria for their use as height references for TanDEM-X. *IEEE Transactions on Geoscience and Remote Sensing* 48 (6), 2750–2757.
- Hueso González, J., Bachmann, M., Hofmann, H., 2010c. TanDEM-X commissioning phase status. In: *Proc. IEEE Geoscience and Remote Sensing Symposium (IGARSS)*, Honolulu, Hawaii, USA, 25–30 July.
- Krieger, G., Moreira, A., Fiedler, H., Hajnsek, I., Werner, M., Younis, M., Zink, M., 2007. TanDEM-X: a satellite formation for high resolution SAR interferometry. *IEEE Transactions on Geoscience and Remote Sensing* 45 (11), 3317–3341.
- Kroes, R., 2006. Precise Relative Positioning of Formation Flying Spacecraft using GPS. PhD Thesis, TU Delft.
- Kroes, R., Montenbruck, O., Bertiger, W., Visser, P., 2005. Precise GRACE baseline determination using GPS. *GPS Solutions* 9 (1), 21–31 (Springer-Verlag GmbH, Heidelberg, Germany).
- Lachaise, M., Fritz, T., Eineder, M., 2008. A new dual baseline phase unwrapping algorithm for the TanDEM-X mission. In: *Proc. of the European SAR Conference (EuSAR)*, Friedrichshafen, Germany, 2–5 June.
- Montenbruck, O., D'Amico, S., Ardaens, J.S., Wermuth, M., 2011. Carrier phase differential GPS for LEO formation flying – the PRISMA and TanDEM-X flight experience. In: *Proc. AAS Astrodynamics Specialist Conference*, Girdwood, USA, 31 July–4 August.
- Schwerdt, M., Hueso González, J., Bachmann, M., Schrank, D., Döring, B., Tous Ramon, N., Walter Antony, J.M., 2011. In-orbit calibration of the TanDEM-X system. In: *Proc. IEEE Geoscience and Remote Sensing Symposium (IGARSS)*, Vancouver, Canada, 24–29 July.
- Zhu, S., Reigber, Ch., König, R., 2004. Integrated adjustment of CHAMP, GRACE, and GPS data. *Journal of Geodesy* 78 (1–2), 103–108.